Proceedings of the 2nd International Symposium
on Adaptive Motion of Animals and Machines,
Kyoto, March.4-8, 2003

Whole-body Cooperative COG Control through ZMP Manipulation for Humanoid Robots

Tomomichi Sugihara†, Yoshihiko Nakamura†,‡

†Univ. of Tokyo, Dept.of Mechano-Informatics, 7–3–1, Hongo, Bunkyo-ku, Tokyo, 113–0033, Japan,
Email: sugihara@ynl.t.u-tokyo.ac.jp

‡Japan Science and Technology Corporation(JST), CREST Program

Abstract

Non-linearity in dynamics of legged robots is so strong that control of them is a quite hard problem. An efficiency of lower-level modelization of robots based on the COG has been confirmed both qualitatively and quantitatively. However, the large gap between such lower-level model and precise model often causes the difficulty. In this paper, COG Jacobian, which relates the whole-body motion to COG motion, is proposed to handle the legged robot. It is also effective for ZMP manipulation which functions as a key for stable and responsive motion. Two applications of it, motion stabilization method based on DTAD(Dual Term Absorption of Disturbance) and VIIP(Variable Impedant Inverted Pendulum) model control, are introduced.

1. Introduction

Complexity of humanoids as dynamical systems lies upon the two issues, namely, i) they are multibody systems with a number of links. Moreover, they are nonholonomic systems in nature, due to having underactuated links. And ii) the structure varies through the interaction with the environment[1]. An appropriate lower-level modelization, therefore, helps to handle such complicated systems.

Miyazaki et al.[2] separated modes of a biped system into slow and fast modes based on singular perturbation. Furusho et al.[3] showed that the behavior of a biped is approximated only by slow modes with a good precision to control with strong local feedback control. The slow modes revealed in these studies are similar to that of an inverted pendulum in accordance with the fact that the COG of the system is located above the working point of external force. Various controlling methods with lower-level models based on this idea have been proposed so far [4, 5, 6].

However, the large gap between the lower-level model and the precise model is the bottleneck since COG is a highly-redundant against the whole joint, it is difficult to resolve the required COG motion into the whole-body motion uniquely. Kajita et al.[4] substituted displacement of the COG for that of trunk, which is only applicable for robots with ignorablly light legs.

In this paper, the concept and calculation method of COG Jacobian of legged systems is proposed. Thanks to it, COG velocity can be controlled just as manipulator endpoint[7]. Tamiya et al.[8] obtained it numerically by quasi-gradient using a kinematic model. It requires a large amount of computation. Furthermore, it does not solve the structure-varying feature. All these difficulties are overcome by the proposed.

It also enables an easy manipulation of the ZMP[9] which is significant in the control of legged systems. The stabilization and responsive motion of them are realized through the manipulation. Two typical applications, motion stabilization method based on DTAD(Dual Term Absorption of Disturbance) and VIIP(Variable Impedant Inverted Pendulum) model control, are introduced to show the efficiency of it.

2. Derivation of COG Jacobian

A legged robot is modelized as is figured in Fig.1; the root link of the robot is connected with the inertia frame Σ_W via a virtual 6-DOF pair, and extremeties branch out of the root. We express the frame bound to the root for Σ_0 hereafter. A velocity vector of arbitrary point $\boldsymbol{p}$ and a rotational velocity of link k, $\boldsymbol{\omega}_k$ can be expressed as follows.

$$\dot{\boldsymbol{p}} = \dot{\boldsymbol{p}}_0 - (\boldsymbol{R}_0{}^0\boldsymbol{p}) \times \boldsymbol{\omega}_0 + \boldsymbol{R}_0{}^0\dot{\boldsymbol{p}} \quad (1)$$

$$\boldsymbol{\omega}_k = \boldsymbol{\omega}_0 + \boldsymbol{R}_0{}^0\boldsymbol{\omega}_k \quad (2)$$

where $\boldsymbol{R}_0$ is an attitude transportation matrix from Σ_0 to Σ_W, $\boldsymbol{p}_0$ is the original point and $\boldsymbol{\omega}_0$ is the rotational velocity of Σ_0 with respect to Σ_W, ${}^0\boldsymbol{\omega}_k$ is a relative rotational velocity of link k and ${}^0\boldsymbol{p}$ is a relative position vector of $\boldsymbol{p}$ with respect to Σ_0. Using the method by

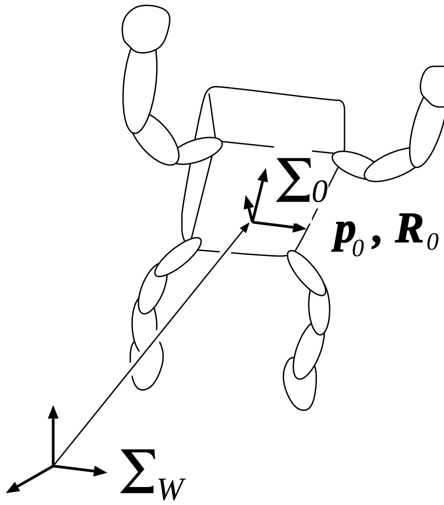

Figure 1: Multi-body Legged Robot

Orin et al.[10], Jacobians ${}^0\boldsymbol{J}_{\omega k}$ and ${}^0\boldsymbol{J}$ which satisfy the following (3)(4) are obtained.

$$ {}^0\dot{\boldsymbol{\omega}}_k = {}^0\boldsymbol{J}_{\omega k}\dot{\boldsymbol{\theta}} \tag{3}$$

$$ {}^0\dot{\boldsymbol{p}} = {}^0\boldsymbol{J}\dot{\boldsymbol{\theta}} \tag{4}$$

From Eq.(1), the COG velocity $\dot{\boldsymbol{p}}_G$ is expressed as:

$$ \dot{\boldsymbol{p}}_G = \dot{\boldsymbol{p}}_0 - (\boldsymbol{R}_0{}^0\boldsymbol{p}_G) \times \boldsymbol{\omega}_0 + \boldsymbol{R}_0{}^0\dot{\boldsymbol{p}}_G \tag{5}$$

${}^0\dot{\boldsymbol{p}}_G$ is calculated as:

$$ {}^0\dot{\boldsymbol{p}}_G = \frac{\sum_{k=1}^{n} m_k{}^0\dot{\boldsymbol{p}}_{Gk}}{\sum_{k=0}^{n} m_k} = \frac{\sum_{k=1}^{n} m_k{}^0\boldsymbol{J}_{Gk}\dot{\boldsymbol{\theta}}}{\sum_{k=1}^{n} m_k} \tag{6}$$

where n is the number of links, m_k is the mass of link k, ${}^0\boldsymbol{p}_{Gk}$ is the COG of link k with respect to Σ_0, $\boldsymbol{\theta}$ is the whole joint angle, and ${}^0\boldsymbol{J}_{Gk}$ is COG Jacobian of each link k. From Eq.(6), we define ${}^0\boldsymbol{J}_G$ as follows.

$$ {}^0\boldsymbol{J}_G \equiv \frac{\sum_{k=1}^{n} m_k{}^0\boldsymbol{J}_{Gk}}{\sum_{k=1}^{n} m_k} \tag{7}$$

Suppose that the link F is fixed in the inertia frame and sufficient friction force prevents it from slipping, both the linear and rotational velocity of link F with respect to Σ_W are zero. Thus, from Eq.(2)(1), we get:

$$ \boldsymbol{\omega}_F = \boldsymbol{0} \Leftrightarrow \boldsymbol{\omega}_0 = -\boldsymbol{R}_0{}^0\boldsymbol{\omega}_F \tag{8}$$

$$ \dot{\boldsymbol{p}}_F = \boldsymbol{0} \Leftrightarrow \dot{\boldsymbol{p}}_0 = (\boldsymbol{R}_0{}^0\boldsymbol{p}_F) \times \boldsymbol{\omega}_0 - \boldsymbol{R}_0{}^0\dot{\boldsymbol{p}}_F \tag{9}$$

where $\boldsymbol{p}_F$ is a certain point in link F. Consequently,

$$ \boldsymbol{\omega}_0 = -\boldsymbol{R}_0{}^0\boldsymbol{J}_{\omega F}\dot{\boldsymbol{\theta}} \tag{10}$$

$$ \dot{\boldsymbol{p}}_0 = -\boldsymbol{R}_0\{{}^0\boldsymbol{p}_F \times ({}^0\boldsymbol{J}_{\omega F}\dot{\boldsymbol{\theta}}) + {}^0\boldsymbol{J}_F\dot{\boldsymbol{\theta}}\} \tag{11}$$

${}^0\boldsymbol{J}_{\omega F}$ and ${}^0\boldsymbol{J}_F$ are obtained from Eq.(3)(4). Putting them into Eq.(5), we get:

$$ \dot{\boldsymbol{p}}_G = \boldsymbol{R}_0\{{}^0\boldsymbol{J}_G - {}^0\boldsymbol{J}_F + [({}^0\boldsymbol{p}_G - {}^0\boldsymbol{p}_F)\times]{}^0\boldsymbol{J}_{\omega F}\}\dot{\boldsymbol{\theta}} \tag{12}$$

where $[\boldsymbol{v}\times]$ corresponding to an arbitrary vector $\boldsymbol{v}$ is an equivalent matrix to the outer product with $\boldsymbol{v}$. From Eq.(12), COG Jacobian $\boldsymbol{J}_G$ can be defined by

$$ \boldsymbol{J}_G = \boldsymbol{R}_0\{{}^0\boldsymbol{J}_G - {}^0\boldsymbol{J}_F + [({}^0\boldsymbol{p}_G - {}^0\boldsymbol{p}_F)\times]{}^0\boldsymbol{J}_{\omega F}\} \tag{13}$$

and it also means that the COG velocity can be related explicitly to the whole joint angle velocity, apparently as the linear summation of it. This fact helps to treat it as a simple linear equational constraint.

3. A Pattern-based Motion Control with DTAD method [11]

3.1. Outline

A pattern-based approach is the easiest way to reduce the difficulty on the control of humanoid robots; operators may prepare proper motion trajectories to accomplish the task, considering the complicated constraints in advance, and simply get robots to replay them. This idea requires online stabilization in addition to designing of the trajectories [12, 13], since various unpredictable factors often make motion of robots unstable in the real world. Though several methods [14, 13, 5] have been proposed, they still have limitation problems of applicability. A stabilization method proposed in this section consists of both the short-term and long-term absorption of disturbance, and thus we named it DTAD(Dual Term Absorption of Disturbance) method. It is applicable for a variety of motion of humanoid robots.

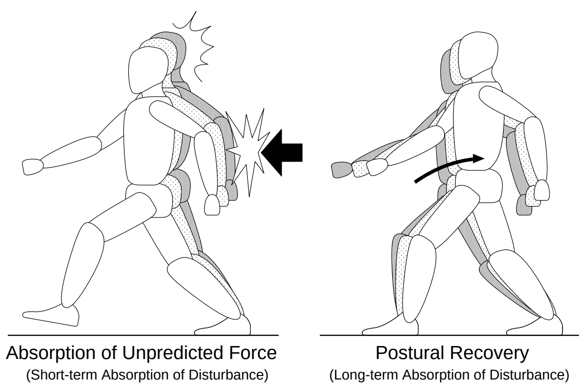

Figure 2: The two basic schemes to balance

Two important schemes exist on the stabilization of legged motion as is figured in Fig.2, that is, i) absorption of unpredicted force, and ii) robust compensation of the postural error. The former item deforms postural pattern, while the latter deforms force pattern, so that they obviously conflict with each other. Human-beings seem to realize such the conflicting schemes with skillful whole-body cooperation. It is expected, therefore, that the implementation of similar function leads to reliable operations of humanoid robots.

Suppose that motion of robots are described by joint angle $\boldsymbol{\theta}$, the COG $\boldsymbol{p}_G = [x_G \ \ y_G \ \ z_G]^T$, the ZMP $\boldsymbol{p}_Z = [x_Z \ \ y_Z \ \ z_Z]^T$, and the vertical reaction force f_z (z-axis coincides with the direction against gravity), and that the command set of the above parameters ${}^{cmd}\boldsymbol{\theta}$, ${}^{cmd}\boldsymbol{x}_G$, ${}^{cmd}\boldsymbol{x}_Z$, ${}^{cmd}f_z$ are given without physical inconsistency. The method proposed calculates as close referential value of $\boldsymbol{\theta}$, ${}^{ref}\boldsymbol{\theta}$ which achieves the two conflicting schemes to ${}^{cmd}\boldsymbol{\theta}$ as possible.

3.2. Short-term Absorption of Disturbance

Unpredicted force often makes motion of robots unstable. Thus, absorption of it is required to avoid short-term crisis. It is achieved by letting $\boldsymbol{p}_Z$ and f_z coincide with ${}^{cmd}\boldsymbol{p}_Z$ and ${}^{cmd}f_z$ respectively. It also works to keep stable contact between the robot and the ground. This should be accomplished in quite short term and we call it *short-term absorption of disturbance*.

Assuming a mass-concentrated model, the equation of motion is approximately expressed as:

$$\ddot{x}_G = \omega^2(x_G - x_Z) \tag{14}$$

$$\ddot{y}_G = \omega^2(y_G - y_Z) \tag{15}$$

$$\ddot{z}_G = \frac{f_z}{m} - g \tag{16}$$

where m is the total mass of the robot, g is the acceleration of gravity, and ω^2 is defined by

$$\omega^2 \equiv \frac{f_z}{m(z_G - z_Z)} \tag{17}$$

Although this ignorance of the inertia of each link makes it less accurate, the amount of computation is reduced enough to be suitable for real-time control. Giving the acceleration in Eq.(14)~(16) with substituting $\boldsymbol{p}_Z$ and f_z for ${}^{cmd}\boldsymbol{p}_Z$ and ${}^{cmd}f_z$ respectively, short-term absorption of disturbance is achieved.

3.3. Long-term Absorption of Disturbance

Modification of acceleration in the previous section 3.2. deforms the postural pattern. In order to recover it, the position of COG should be put back to the desired position. It is realized by substituting ${}^{cmd}\boldsymbol{p}_Z$ and ${}^{cmd}f_z$ for the following ${}^{ref}\boldsymbol{p}_Z$ and ${}^{cmd}f_z$ respectively.

$${}^{ref}x_Z = {}^{cmd}x_Z - K_x\Delta^{cmd}x_G + D_x\Delta^{cmd}\dot{x}_G \tag{18}$$

$${}^{ref}y_Z = {}^{cmd}y_Z - K_y\Delta^{cmd}y_G + D_y\Delta^{cmd}\dot{y}_G \tag{19}$$

$${}^{ref}f_z = {}^{cmd}f_z + m(K_z\Delta^{cmd}z_G + D_z\Delta^{cmd}\dot{z}_G) \tag{20}$$

where K_* and D_* are the proportional and differential gains respectively, and $\Delta^{cmd}*_G$ is defined by

$$\Delta^{cmd}*_G \equiv {}^{cmd}*_G - *_G \tag{21}$$

Since the ZMP has to be located in a certain region and the ground reaction force has to be positive, when ${}^{ref}\boldsymbol{p}_Z$ and ${}^{ref}f_z$ don't satisfy these conditions, the nearest value within the region is chosen instead.

This procedure should be accomplished in rather long term than short-term absorption of disturbance so that we call it *long-term absorption of disturbance*. Conclusively, ${}^{ref}\ddot{\boldsymbol{p}}_G$ is decided from Eq.(14)~(16) and (18)~(20). Integrating it, we get ${}^{ref}\dot{\boldsymbol{p}}_G$.

3.4. COG Control with Whole-body Cooperation

${}^{ref}\boldsymbol{\theta}$ should be as close value to ${}^{cmd}\boldsymbol{\theta}$ as possible. This problem can be interpreted to the following.

$$\frac{1}{2}({}^{cmd}\dot{\boldsymbol{\theta}} - {}^{ref}\dot{\boldsymbol{\theta}})^T \boldsymbol{W}({}^{cmd}\dot{\boldsymbol{\theta}} - {}^{ref}\dot{\boldsymbol{\theta}}) \longrightarrow \text{min.}$$
$$\text{subject to} \begin{cases} \boldsymbol{J}_G{}^{ref}\dot{\boldsymbol{\theta}} = {}^{ref}\dot{\boldsymbol{p}}_G \\ \boldsymbol{J}_C{}^{ref}\dot{\boldsymbol{\theta}} = \boldsymbol{c} \end{cases} \Leftrightarrow \boldsymbol{J}_U{}^{ref}\dot{\boldsymbol{\theta}} = \boldsymbol{u} \tag{22}$$

where $\boldsymbol{W}$ is the weighting matrix and $\boldsymbol{J}_C{}^{ref}\dot{\boldsymbol{\theta}} = \boldsymbol{c}$ means the constraint required for the task execution.

(22) can be solved as:

$${}^{ref}\dot{\boldsymbol{\theta}} = {}^{cmd}\dot{\boldsymbol{\theta}} + \boldsymbol{W}^{-1}\boldsymbol{J}_U^T(\boldsymbol{J}_U\boldsymbol{W}^{-1}\boldsymbol{J}_U^T)^{-1}\boldsymbol{v} \tag{23}$$
$$\boldsymbol{v} \equiv \boldsymbol{J}_U{}^{cmd}\dot{\boldsymbol{\theta}} - \boldsymbol{u}_i$$

Each joint angle actuator is controlled according to ${}^{ref}\dot{\boldsymbol{\theta}}$. Then, the whole-body motion of the robot is achieved. Giving an adequate $\boldsymbol{W}$, an effective whole-body cooperative motion stabilization is achieved.

3.5. Simulation

We verified the method in some simulations, using a model of HOAP-1(Fujitsu Automation Ltd.). Kinematic structure, size and mass of the robot are shown in Fig.5. Fig.3 is a snapshot of walking motion under impulsive disturbance. Fig.4 shows the loci of each component of the COG. These figure the method proposed works as is expected, stabilizing the motion with the whole-body cooperation.

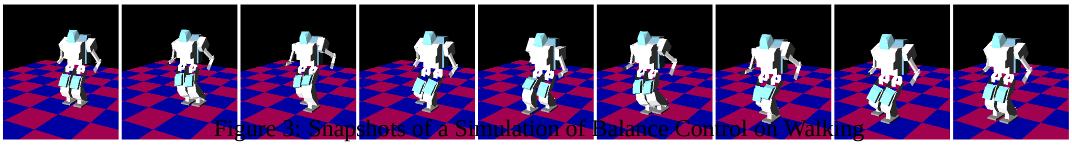

Figure 3: Snapshots of a Simulation of Balance Control on Walking

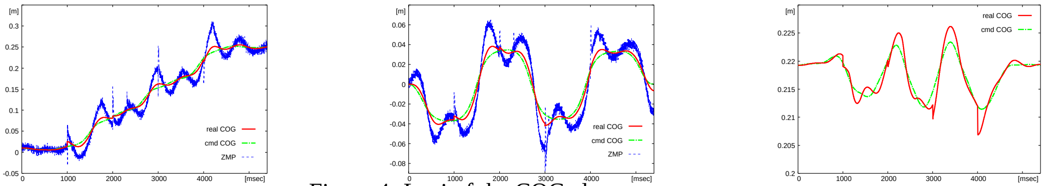

Figure 4: Loci of the COG along x, y, z axes

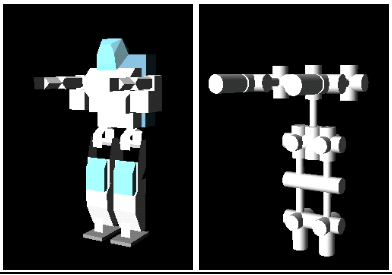

DOF:	20 (8 for arm,12 for leg)
height:	480 [mm]
weight:	6.5 [kg]

Figure 5: Kinematic structure, Size and mass of the robot

4. Motion Control based on VIIP [15]

4.1. Outline

Though pattern-based approaches can reduce the difficulty in realizing a variety of motion, they are less promissing in the real environment filled with unpredictable factors. A controlling method for much more responsive motion is required. Previous trials[16, 6], however, commonly suffer from the complexity of the problem. VIIP(Variable Impedant Inverted Pendulum) model control can give a solution of it.

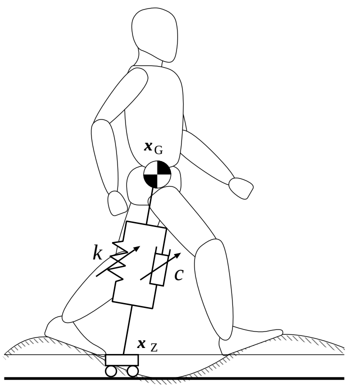

Figure 6: Legged system and VIIP model

One can see from Eq.(14) and (15) that legged robots have similar dynamics with an inverted pendulum whose supporting point is equivalently located at the ZMP. Thus, the COG can be controlled as well as an inverted pendulum through ZMP manipulation.

The supporting point of an inverted pendulum can be manipulated directly, while ZMP cannot. Giving the acceleration in Eq.(14)∼(16), however, to the COG with $\boldsymbol{p}_Z$ and f_z substituted for ${}^{ref}\boldsymbol{p}_Z$ and ${}^{ref}f_z$ respectively, it becomes manipulable indirectly. Integrating it, the referential COG velocity ${}^{ref}\dot{\boldsymbol{p}}_G$ is calculated.

Suppose the referential COG velocity is given as ${}^{ref}\boldsymbol{v}_G$. ${}^{ref}\boldsymbol{p}_Z$ is decided as an actuating value by any common controlling method for inverted pendulums in order to let $\dot{\boldsymbol{p}}_G$ converge to ${}^{ref}\boldsymbol{v}_G$. In the case that ${}^{ref}\boldsymbol{p}_Z$ is out of the supporting region, just the same way with that in 3.3. is adopted.

${}^{ref}f_z$ should be decided independently from ${}^{ref}\boldsymbol{p}_Z$. Adequate decision of this value enables the robot to act more adaptive and responsive, or even to transit seamlessly from/to contact phase to/from aerial phase. Here, we decide ${}^{ref}f_z$ as:

$$ {}^{ref}f_z = K_{Pz}({}^{ref}z_G - z_G) + K_{Dz}({}^{ref}\dot{z}_G - \dot{z}_G) + mg \quad (24) $$

K_{Pz} and K_{Dz} are decided in accordance with the current contact state and the motion scheme. The COG height z_G converges to ${}^{ref}z_G$ without overshoot when K_{Pz} and K_{Dz} satisfy the following condition.

$$ K_{Pz} > 0, \quad K_{Dz} > 0, \quad K_{Dz}^2 - 4K_{Pz} > 0 \quad (25) $$

Lifting-off motion is achieved by giving enough velocity and acceleration against the gravity to the COG. Then, K_{Pz} and K_{Dz} are designed as:

$$ K_{Dz} = 0, \quad K_{Pz} = \frac{2mgz_H}{z_d^2} \quad (26) $$

where z_H and z_d is a planned maximum height and a planned stooping depth from ${}^{ref}z_G$ respectively. Conversely, in order to absorb the impact at the moment of touchdown, K_{Pz} and K_{Dz} are designed as:

$$K_{Dz} = 0, \quad K_{Pz} = \frac{m\dot{z}_{G-}^2}{z_d^2} \tag{27}$$

where $\dot{z}_{G-}$ is the falling speed immediately before touchdown, and z_d is a planned stooping depth after touchdown. Fig.6 illustrates this modelization of VIIP.

4.2. Synergetic Generation of Whole-body Motion

Resolution of ${}^{ref}\dot{\boldsymbol{p}}_G$ is done by arranging (22) as:

$$\begin{gathered} \frac{1}{2}{}^{ref}\dot{\boldsymbol{\theta}}^T \boldsymbol{W} {}^{ref}\dot{\boldsymbol{\theta}} \longrightarrow \text{min.} \\ \text{subject to} \begin{cases} \boldsymbol{J}_G {}^{ref}\dot{\boldsymbol{\theta}} = {}^{ref}\dot{\boldsymbol{p}}_G \\ \boldsymbol{J}_C {}^{ref}\dot{\boldsymbol{\theta}} = \boldsymbol{c} \end{cases} \Leftrightarrow \boldsymbol{J}_U {}^{ref}\dot{\boldsymbol{\theta}} = \boldsymbol{u} \end{gathered} \tag{28}$$

and the solution is

$${}^{ref}\dot{\boldsymbol{\theta}} = \boldsymbol{W}^{-1}\boldsymbol{J}_U^T(\boldsymbol{J}_U\boldsymbol{W}^{-1}\boldsymbol{J}_U^T)^{-1}\boldsymbol{u} \tag{29}$$

The success of this simple management of such the complex system underlies the same principle with *synergetics* known in a biological field; many natural systems with a large number of DOFs act in accordance with constraints which reduces the apparent DOF.

4.3. Simulation

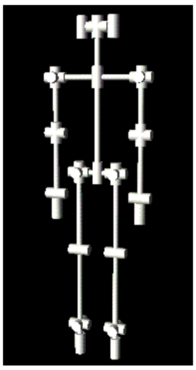

DOF:	30
	(4 for head)
	(14 for arm)
	(12 for leg)
height:	1270 [mm]
weight:	35 [kg]

Figure 11: Kinematic structure, size and mass of the robot

We confirmed the validity of the proposed through some computer simulations as i) the COG displacement on both feet, ii) stepping motion and iii) one-step-forward motion and walking. Fig.11 shows kinematic structure, size and mass properties of the robot model.

A stepping motion with impulsive disturbance has also been examined. Fig.7 is a snapshot. The robot moved adaptively to cope with disturbance. Fig.8 is the loci of $\boldsymbol{p}_G$, ${}^{ref}\boldsymbol{p}_Z$ and $\boldsymbol{p}_Z$ with respect to Σ_0, which shows that $\boldsymbol{p}_Z$ follows ${}^{ref}\boldsymbol{p}_Z$ with a good accuracy.

A jumping motion by HOAP-1 model is also realized in a simulation. Fig.9 is a snapshot of the motion. And the loci of both COG and ZMP are shown in Fig.10. We've verified that the method works properly and the stable jumping motion is achieved.

5. Conclusion

COG Jacobian to evade dynamical complexity of the legged systems and handle them is derived. A stabilization method based on DTAD and VIIP model control to realize responsive motion are introduced as its applications. They are achieved through ZMP manipulation, which is also enabled with COG Jacobian.

Acknowledgments

This research was supported by the "Robot Brain Project" under the Core Research for Evolutional Science and Technology (CREST program) of the Japan Science and Technology Corporation (JST).

References

[1] Y.Nakamura and K.Yamane. Dynamics Computation of Structure-Varying Kinematic Chains and Its Application to Human Figures. *IEEE Transactions on Robotics and Automation*, 16(2):124–134, 2000.

[2] F.Miyazaki and S.Arimoto. A Control Theoretic Study on Dynamical Biped Locomotion. *Transaction of the ASME, Journal of Dynamic Systems, Measurement, and Control*, 102:233–239, 1980.

[3] J.Furusho and M.Masubuchi. Control of a dynamical biped locomotion system for steady walking. *Transactions of the ASME, Journal of Dynamic Systems, Measurement, and Control*, 108:111–118, 1986.

[4] S.Kajita and K.Tani. Experimental Study of Biped Dynamic Walking in the Linear Inverted Pendulum Mode. In *Proc. of the 1995 IEEE Int. Conf. on Robotics & Automation*, pages 2885–2819, 1995.

[5] Kazuo Hirai et al. The Development of Honda Humanoid Robot. In *Proc. of the 1998 IEEE Int. Conf. on Robotics & Automation*, pages 1321–1326, 1998.

[6] Hiroki Takeuchi. Development of "MEL HORSE". In *Proc. of the 2001 IEEE Int. Conf. on Robotics & Automation*, pages 3165–3171, 2001.

[7] D.E.Whiteny. Resolved Motion Rate Control of Manipulators and Human Prostheses. *IEEE Transactions on Man-Machine Systems*, 10(2):47–53, 1969.

[8] S.Kagami et al. AutoBalancer: An Online Dynamic Balance Compensation Scheme for Humanoid Robots. In *Proc. of the 4th Int. Workshop on Algorithmic Foundation on Robotics*, 2000.

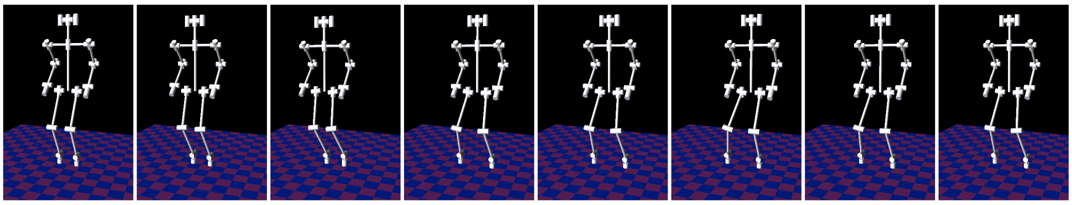

Figure 7: A stepping motion with an impact

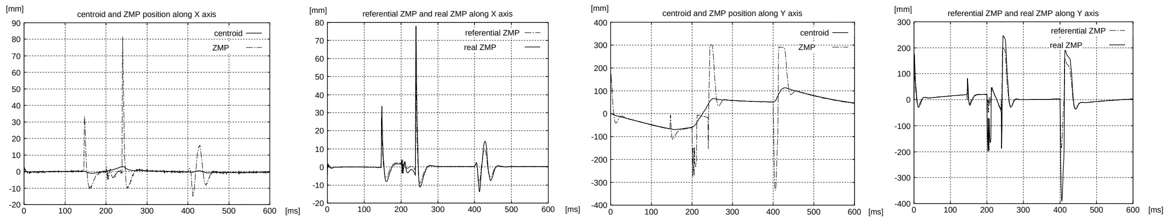

Figure 8: Loci of the COG, the referential ZMP and the real ZMP

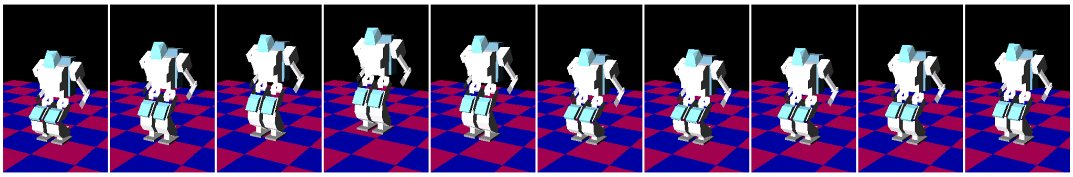

Figure 9: Snapshot of a jump motion simulation

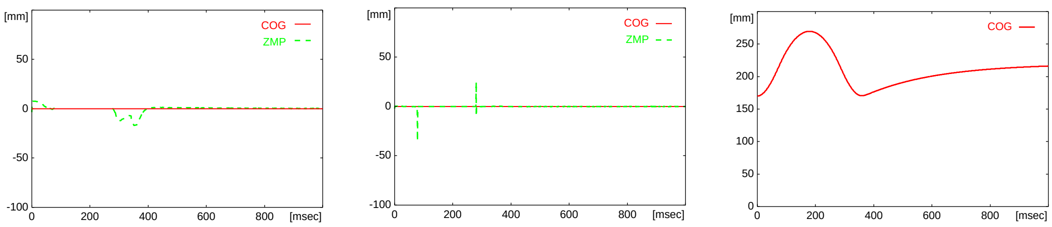

x-axis y-axis z-axis

Figure 10: Loci of COG and ZMP in each axis

[9] M.Vukobratović and J.Stepanenko. On the Stability of Anthropomorphic Systems. *Mathematical Biosciences*, 15(1):1–37, 1972.

[10] D.E.Orin and W.W.Schrader. Efficient Computation of the Jacobian for Robot Manipulators. *The International Journal of Robotics Research*, 3(4):66–75, 1984.

[11] T.Sugihara and Y.Nakamura. Whole-body Cooperative Balancing of Humanoid Robot using COG Jacobian. In *Proc. of the 2002 IEEE/RSJ Int. Conf. on Intelligent Robots and Systems*, 2002.

[12] Jin'ichi Yamaguchi et al. Development of a Bipedal Humanoid Robot – Control Method of Whole Body Cooperative Dynamic Biped Walking –. In *Proc. of the 1999 IEEE Int. Conf. on Robotics & Automation*, pages 368–374, 1999.

[13] Ken'ichiro Nagasaka. *The Whole-body Motion Generation of Humanoid robot Using Dynamics Filter(Japanese)*. PhD thesis, Univ. of Tokyo, 2000.

[14] J.H.Park and H.C.Cho. An On-Line Trajectory Modifier for the Base Link of Biped Robots To Enhance Locomotion Stability. In *Proc. of the 2000 IEEE Int. Conf. on Robotics & Automation*, pages 3353–3358, 2000.

[15] Tomomichi Sugihara et al. Realtime Humanoid Motion Generation through ZMP Manipulation based on Inverted Pendulum Control. In *Proc. of the 2002 IEEE Int. Conf. on Robotics & Automation*, pages 1404–1409, 2002.

[16] A.Kawamura Y.Fujimoto. Simulation of an Autonomous Biped Walking Robot Including Environmental Force Interaction. *IEEE Robotics & Automation Magazine*, 5(2):33–41, 1998.